



Published in final edited form as:

Ann N Y Acad Sci. 2009 May ; 1166: 112–119. doi:10.1111/j.1749-6632.2009.04520.x.

## ***Ixodes ovatus* Ehrlichia Exhibits Unique Ultrastructural Characteristics in Mammalian Endothelial and Tick-derived Cells**

Ulrike G. Munderloh<sup>a</sup>, David J. Silverman<sup>b</sup>, Katherine C. MacNamara<sup>d</sup>, Gilbert G. Ahlstrand<sup>c</sup>, Madhumouli Chatterjee<sup>d</sup>, and Gary M. Winslow<sup>d</sup>

<sup>a</sup>Department of Entomology, University of Minnesota, St. Paul, Minnesota 55108, USA

<sup>b</sup>Department of Microbiology and Immunology, University of Maryland School of Medicine, Baltimore, Maryland 21201, USA

<sup>c</sup>Imaging Center, University of Minnesota, St. Paul, Minnesota 55108, USA

<sup>d</sup>Wadsworth Center, New York State Department of Health, Albany, New York 12208, USA

### **Abstract**

Tick-borne pathogens in the genus *Ehrlichia* cause emerging zoonoses. Although laboratory mice are susceptible to *Ehrlichia* infections, many isolates do not cause clinical illness. In contrast, the *Ixodes ovatus* *Ehrlichia*-like agent (IOE) causes disease and immune responses in mice comparable to the human illness caused by *Ehrlichia chaffeensis*. No culture system had been developed for IOE, however, which limited studies of this pathogen. We reasoned that endothelial and tick cell lines could potentially serve as host cells, since the IOE is found in ticks and in endothelial cells in mice. Infected spleen cells from RAG-deficient mice were overlaid onto ISE6 and RF/6A cultures, and colonies typical of *Ehrlichia* were noted in RF/6A cells within 2 weeks. Infection of ISE6 cells was established after transfer of IOE from RF/6A cells. Electron microscopy revealed densely packed inclusions in infected RF/6A and ISE6 cells; these inclusions contained copious amounts of filamentous structures, apparently originating from *Ehrlichial* cells. In particular, within RF/6A cells the structures assumed an ordered morphology of finely combed hair. IOE from RF/6A cells, when inoculated into C57BL/6 and RAG-deficient mice, induced fatal disease. These data reveal unique structural features of IOE that may contribute to the pathogen's high virulence.

### **Keywords**

*Ehrlichia*; tick cell; endothelial cell; bacterial infection; ultrastructure

### **Introduction**

The ehrlichiae comprise a genus of obligate intracellular bacteria within the family *Anaplasmataceae*.<sup>1</sup> Propagation of these agents requires that the bacteria infect and multiply within eukaryotic cells. Since the ehrlichiae are well-known to reside in macrophages and other phagocytic blood cells (e.g., *E. ewingii* infects neutrophils and eosinophils),

© 2009 New York Academy of Sciences

Address for correspondence: Gary Winslow, Wadsworth Center, 120 New Scotland Avenue, Albany, NY 12208. Voice: +518-473-2795; fax: +518-486-9858. gary.winslow@wadsworth.org.

The authors have no competing financial interests.

**Conflicts of Interest** The authors declare no conflicts of interest.

propagation is commonly performed in human myelomonocytic cell lines such as HL-60,<sup>2</sup> or in macrophage cell lines such as DH82<sup>3</sup> and THP-1 cells.<sup>4</sup> Although many of the ehrlichiae have been cultured from clinical isolates or laboratory-infected mice, establishment of these organisms in cell lines has often been difficult, and some isolates have resisted culturing. Among these is the *Ixodes ovatus Ehrlichia*-like agent, IOE, a bacterium identical or closely related to "*Candidatus Neoehrlichia mikurensis*."<sup>5</sup> IOE was originally identified in *Ixodes ovatus* ticks in Japan and was shown to fatally infect mice.<sup>6</sup> IOE is a particularly pathogenic ehrlichia that can induce a fatal disease in mice that resembles human monocytotropic ehrlichiosis.<sup>7,8</sup> Thus, the bacterial isolate has provided a very useful model for examination of aspects of immunity and immunopathology.<sup>9-14</sup> Until now, however, it had not been possible to culture IOE, and passage of the bacteria in mice has been necessary; this limitation has precluded detailed genetic and ultrastructural analyses. Since IOE has been shown to infect not only monocytic cells, but also endothelial cells and macrophages, we reasoned that non-myelomonocytic cell lines would be good candidates for *in vitro* culture. In this study, we demonstrate the culture of IOE in the rhesus monkey (*Macaca mulatta*) endothelial cell line RF/6A,<sup>15</sup> and in the tick cell line ISE6.<sup>16</sup> Furthermore, our data reveal unique ultrastructural features of IOE that may be associated with the organism's high virulence in laboratory mice.

## Materials and Methods

### Cell Culture

RF/6A cells were obtained from the American Tissue Type Culture Association (ATCC, Manassas, VA, USA; ATCC CRL-1780) and were cultured in L15B300<sup>16</sup> supplemented with 5% FBS (heat-inactivated; Harlan, Indianapolis, IN, USA), 5% TPB (Difco, Detroit, MI, USA), 0.1% lipoprotein concentrate (MP Biomedical, Irvine, CA, USA), 25 mM HEPES, 0.25% NaHCO<sub>3</sub>, adjusted to pH ~7.5, in the absence of antibiotics at 37°C in a 5% CO<sub>2</sub>-atmosphere. The tick cell line ISE6 was routinely propagated in the same medium, but without HEPES and NaHCO<sub>3</sub>, in tightly capped flasks at 34°C. For IOE culture, however, 25 mM HEPES and 0.25% NaHCO<sub>3</sub> were included in tick cell culture medium as well, as described.<sup>16</sup> Subsequent passage of RF/6A was performed in Complete Tumor Medium, as described previously.<sup>17</sup>

### IOE and *Ehrlichia muris* Isolation

IOE and *Ehrlichia muris* were obtained from spleens of infected C57BL/6 RAG-deficient mice on day 9 post-infection. Spleen tissue was mechanically disrupted, erythrocytes were lysed, and mononuclear cells were suspended in Complete Tumor Medium.<sup>17</sup> Splenocytes were collected by centrifugation at 1000 × g for 15 min., and resuspended in L15B300 supplemented as stated above; spleen cells infected with either *Ehrlichia* species were then overlaid separately on RF/6A and ISE6 cell cultures. Antibiotics and antifungals were not used. Quantitative PCR analyses indicated that the spleen cell suspension contained 8.2 × 10<sup>4</sup> IOE copies per 10 ng total DNA (equivalent to approximately 2000 host cells).

### Ultrastructural Analyses

Cells in culture were prepared for electron microscopy when the cultures were approximately 70–90% infected. After removal of the growth medium, cell layers were flooded with modified Ito's fixative,<sup>18</sup> and fixed for 15 min. on ice. Cells were carefully scraped off the substrate, collected by centrifugation at 100×g for 10 min, and resuspended in fresh fixative. After washing 3 times by centrifugation in phosphate buffer, pH 7.2, the cells were post-fixed in 1% osmium tetroxide in sodium phosphate buffer, pH 7.2 for 1 hr at room temperature, dehydrated in an ascending ethanol series and embedded in Epon 812. Ultrathin sections were cut on a Sorvall MT-1 ultramicrotome, stained with uranyl acetate

and lead citrate, and examined and photographed in a JEOL 1200 EX or FEI CM12 electron microscope operating at 60 kV.

### Light Microscopy

To confirm infection, we centrifuged infected cells onto microscope slides (Cytospin, Shandon Southern Instruments, Sewickley, PA), fixed them in methanol, and stained them with Giemsa's solution. Preparations were examined with an Olympus BH2 microscope, and images were captured with a Scion Greyscale digital camera (model CFW-1310M) and Scion Visicapture software (Scion Corporation, Frederick, MD, USA) running on an Apple iMac (Apple Computer, Inc., Cupertino, CA, USA).

### Immunofluorescence Detection

The IOE cultured in the RF/6A were detected using a biotinylated anti-OMP-19 antibody (Ec18.1<sup>19</sup>) followed by streptavidin-Alexa-fluor 488 (Molecular Probes, Invitrogen, Carlsbad, CA, USA). The cells were permeabilized with 0.1% saponin and nonspecific binding was inhibited with a streptavidin-biotin blocking kit (Vector Laboratories, Burlingame, CA, USA).

### Mice and Infections

C57BL/6 and C57BL/6-Rag1<sup>tm1Mom</sup>/J mice were obtained from Jackson Laboratories (Bar Harbor, ME, USA) and were maintained in the Animal Care Facility at the Wadsworth Center under microisolator conditions in accordance with institutional guidelines for animal welfare. Mice were gender-matched for each experiment and were 6 to 12 weeks in age. For infections, RF/6A cells were harvested from infected cultures using a cell scraper and disrupted using a Braun-Sonic 2000 sonicator (40 W for 2 mins on ice). The cell lysate was clarified by low-speed centrifugation (600 × g), and the bacteria were harvested by high-speed centrifugation (10,000 × g). The pelleted bacteria were resuspended in sucrose-phosphate-glutamate (SPG) buffer (0.0038 M KH<sub>2</sub>PO<sub>4</sub>/0.0072 M K<sub>2</sub>HPO<sub>4</sub>/0.0049 M L-glutamate-0.218M sucrose, pH 7.2) and injected intraperitoneally into mice. Moribund mice judged to be incapable of surviving infection; indicated by ruffled coat, immobility, and hunched posture, and were humanely sacrificed.

## Results

### Infection of RF/6A and ISE6 Cells with IOE and *E. muris*

Of the primary cultures initially seeded with IOE or *E. muris*-infected splenocytes, one RF/6A and one ISE6 culture of IOE, as well as one ISE6 culture of *E. muris*, appeared to be productively infected and were chosen for expansion. Productive infection with IOE was first noted in RF/6A cells by phase contrast microscopy of intact cell layers 2 weeks after addition of IOE obtained from spleen cells from a RAG-deficient C57BL/6 mouse. Initially, inclusions suggestive of ehrlichial morulae were small, and there usually were several in each infected cell. These subsequently grew until the entire cytoplasm was filled with numerous bacteria. Giemsa-stained cell spreads confirmed the presence of multiple small IOE-morulae in RF/6A rhesus endothelial cells (Fig. 1A) and ISE6 tick cells (Fig. 1B). Notably, IOE within tick cells clustered inside their inclusion, leaving an apparently empty "halo" around the bacteria; the halo could also be seen in live cultures (data not shown). In contrast, *E. muris* produced one or two large inclusions in each tick cell (Fig. 1C). No IOE were recovered from the primary culture of ISE6 tick cells, but subsequent passage of IOE from RF/6A to ISE6 cells was successful. Although IOE were originally isolated in RF/6A cells with L15B300, they were later propagated successfully in RPMI1640 with 25 mM HEPES buffer and 10% heat-inactivated FBS, and in Complete Tumor Medium composed

of Eagle's MEM supplemented with 10  $\mu$ M 2-mercaptoethanol, 10% Mishell-Dutton Nutrient cocktail,<sup>20</sup> and 10% FBS.

Electron microscopic analyses revealed an accumulation of copious amounts of fibrillar material in IOE morulae. This appearance was most striking in RF/6A cells, where the material displayed an orderly appearance of fine, combed hair (Fig. 2A, B). The structures seemed to be streaming from the bacteria, obscuring details of their cell wall in most cases, and individual bacteria were extremely pleomorphic and condensed to varying degrees. In tick cells also (Fig. 2C), fibrillar material was evident inside the inclusions, but, here, it was arranged in a disorganized, random fashion. The inset in Figure 2, panel C, shows a cross section of an individual bacterium, revealing the typical structure of the ehrlichial cell wall.<sup>5</sup> For comparison, sections of *E. muris*-infected ISE6 tick cells are shown in panels D and E. The *E. muris* morulae lacked fibrillar material, and ehrlichiae were only moderately pleomorphic compared to IOE. The *E. muris* bacteria had an ultrastructural organization typical of organisms in the genus *Ehrlichia*. The inclusions in panel D contain a mixture of reticulated and dense core forms, while the inclusions in panel E are entirely composed of reticulated organisms bounded by flaccid membranes.

### IOE Cultured in RF/6A Cells Retained Antigenicity

To confirm that the cultured IOE retain antigenicity, immunohistochemical analyses of the IOE in RF/6A cells, was performed with the anti-OMP-19 antibody Ec18.1.<sup>19</sup> Although the antibody was raised against OMP-19 from *E. chaffeensis*, the antibody epitope is conserved in IOE.<sup>21</sup> Infected cells containing many morulae were detected, indicating that OMP-19 expression was maintained in the endothelial cell line (Fig. 3).

### IOE Cultured in RF/6A Cells Is Fully Competent to Infect Immunocompromised and Immunocompetent Mice

IOE grown in RF/6A cells readily infected C57BL/6 and RAG-deficient mice and caused mortality within 9–14 days post-infection, as observed in previous studies that used mouse-passaged bacteria.<sup>9,14</sup> For confirmation that the IOE grown in RF/6A cells were infectious, cell-free ehrlichiae obtained after ultrasonic disruption were used to infect C57BL/6 RAG-deficient mice via the peritoneum. Retrospective quantitative PCR analyses revealed that mice were infected with a range of 4–6 log<sub>10</sub> bacterial copies. All RAG-deficient infected mice were judged to be moribund and incapable of surviving infection within 9 days post-infection, indicating that the RF/6A-grown bacteria were fully infectious (Fig. 4). Similar inoculations performed with C57BL/6 mice also induced fatal disease (data not shown). Bacteria isolated from the spleens of infected RAG-deficient mice were successfully recultured *in vitro* in RF/6A cells (data not shown).

## Discussion

The present report details the successful culture of the IOE agent *in vitro*. This accomplishment will facilitate research that entails the use of large numbers of purified bacteria, such as genetic transformation and analysis, and biochemical studies. Even though methods are becoming more widely used that permit analysis of the behavior of pathogens *in vivo* (e.g., tissue-specific gene expression assays using quantitative reverse transcription PCR), studies that utilize large numbers of pure microbes typically require a source of bacteria from *in vitro* cultures. In addition, cell culture provides an opportunity to observe the organisms in a living state or with minimal manipulation. Although myelomonocytic cells are often considered to be the chief targets of IOE and related ehrlichiae *in vivo*, IOE are known to infect cell types, including endothelial cells and hepatocytes.<sup>22</sup> This likely explains the ability of IOE to establish infection in the rhesus monkey endothelial cell line

RF/6A and suggests that other endothelial cell lines could be susceptible to infection. RF/6A also supported the growth of related tick-borne pathogens (i.e., *Anaplasma phagocytophilum* and *A. marginale*),<sup>23</sup> and, thus, it may be broadly suitable for other *Anaplasma*. Since endothelial cells can present major histo-compatibility complex (MHC) processed peptide antigens, infecting bacteria could potentially interfere with this pathway, thereby altering the immune response in the pathogen's favor.<sup>24</sup> We conclude that endothelial cell cultures provide a relevant and useful *in vitro* model whose utilization will facilitate investigation of the biology, pathogenesis, and immunological aspects of infection with the IOE and related bacteria.

Culture was also successful in the tick-derived cell line ISE6, a line that has been used to propagate other *Ehrlichia* and *Anaplasma* species.<sup>16,25</sup> In those cases, however, IOE were not recovered in tick cells from the primary in oculum of infected blood, but only after transfer from RF/6A cells. Whether that result was due to the prior mouse-to-mouse passage history of the isolate and concomitant adaptation to the mammalian host, or whether it reflected a lower degree of susceptibility of the tick cells relative to the RF/6A cells, will require additional investigation. Regardless, the availability of two culture systems representing both the mammalian host and the arthropod vector will benefit studies that seek to examine the entire life cycle of the IOE *in vitro*, and those that focus on IOE in either the mammal or the tick. It is likely that the IOE differentially expresses specific subsets of genes or gene variants necessary for survival in cells from these very different hosts, as has been shown to be the case for related pathogens.<sup>25,26</sup> This assumption is supported by the different appearances of the IOE between tick cells and mammalian cells (see Figs. 1A, B and 2A, B, and C). Notably, in RF/6A cells, the bacteria filled the entire inclusion, whereas in ISE6 tick cells, some of the inclusions showed a clear zone next to or surrounding a group of IOE. The most striking feature, visible upon electron microscopic examination of sectioned material, was a matrix of regularly arrayed fibrils embedding the IOE. In places, these converged into dense bundles (see Fig. 2A, arrows). Although IOE morulae within tick cells also contained an undefined material admixed in with the bacteria, such material was irregular and stringy and flocculent in appearance, quite unlike the highly structured fibrils seen in RF/6A cells. *Ehrlichia muris*, grown in ISE6 cells under identical conditions and processed at the same time and in the same manner, did not contain such material in their morulae, suggesting that it was unique to the IOE. The function of these structures, especially in the RF/6A cells, remains unknown. Other investigators have demonstrated the presence of amorphous material among *E. chaffeensis* inside morulae,<sup>27-29</sup> but none of those studies documented the highly regularly structured fibrils described here. We propose that they are a unique feature of the biology of IOE and are possibly linked to the organism's high pathogenicity in mice.

## Acknowledgments

The authors wish to thank Kathryn Hogle and Shelia Le of the Wadsworth Center for excellent technical assistance, and the Wadsworth Center Animal Care Facility.

This work was supported by US Public Health Service grant R01AI47963-01 to GMW and R01 AI042792-09 to UGM.

## References

1. Dumler JS, et al. Reorganization of genera in the families Rickettsiaceae and Anaplasmataceae in the order Rickettsiales: Unification of some species of *Ehrlichia* with *Anaplasma*, *Cowdria* with *Ehrlichia* and *Ehrlichia* with *Neorickettsia*, descriptions of six new species combinations and designation of *Ehrlichia equi* and 'HGE agent' as subjective synonyms of *Ehrlichia phagocytophila*. *Int. J. Syst. Evol. Microbiol.* 2001; 51:2145–2165. [PubMed: 11760958]



2. Goodman JL, et al. Direct cultivation of the causative agent of human granulocytic ehrlichiosis. *N. Engl. J. Med.* 1996; 334:209–215. [PubMed: 8531996]
3. Heimer R, Tisdale D, Dawson JE. A single tissue culture system for the propagation of the agents of the human ehrlichioses. *Am. J. Trop. Med. Hyg.* 1998; 58:812–815. [PubMed: 9660470]
4. Barnewall RE, Rikihisa Y. Abrogation of gamma interferon-induced inhibition of *Ehrlichia chaffeensis* infection in human monocytes with iron transferrin. *Infect. Immun.* 1994; 62:4804–4810. [PubMed: 7927758]
5. Kawahara M, et al. Ultrastructure and phylogenetic analysis of '*Candidatus Neoehrlichia mikurensis*' in the family Anaplasmataceae, isolated from wild rats and found in *Ixodes ovatus* ticks. *Int. J. Syst. Evol. Microbiol.* 2004; 54:1837–1843. [PubMed: 15388752]
6. Shibata S, et al. New Ehrlichia species closely related to *Ehrlichia chaffeensis* isolated from *Ixodes ovatus* ticks in Japan. *J. Clin. Microbiol.* 2000; 38:1331–1338. [PubMed: 10747103]
7. Okada H, et al. Distribution of Ehrlichiae in tissues as determined by in-situ hybridization. *J. Comp. Pathol.* 2003; 128:182–187. [PubMed: 12634096]
8. Okada H, et al. Ehrlichial proliferation and acute hepatocellular necrosis in immunocompetent mice experimentally infected with the HF strain of Ehrlichia, closely related to *Ehrlichia chaffeensis*. *J. Comp. Pathol.* 2001; 124:165–171. [PubMed: 11222014]
9. Ismail N, et al. Overproduction of TNF-alpha by CD8+ type 1 cells and down-regulation of IFN-gamma production by CD4+ Th1 cells contribute to toxic shock-like syndrome in an animal model of fatal monocytotropic ehrlichiosis. *J. Immunol.* 2004; 172:1786–1800. [PubMed: 14734762]
10. Ismail N, Stevenson HL, Walker DH. Role of tumor necrosis factor alpha (TNF- $\alpha$ ) and interleukin-10 in the pathogenesis of severe murine monocytotropic ehrlichiosis: Increased resistance of TNF Receptor p55- and p75-deficient mice to fatal ehrlichial infection. *Infect. Immun.* 2006; 74:1846–1856. [PubMed: 16495559]
11. Stevenson HL, et al. An intradermal environment promotes a protective type-1 response against lethal systemic monocytotropic ehrlichial infection. *Infect. Immun.* 2006; 74:4856–4864. [PubMed: 16861674]
12. Bitsaktsis B, Nandi B, Winslow G. T Cell-independent humoral immunity is sufficient for protection against fatal intracellular ehrlichia infection. *Infect. Immun.* 2007; 75:4933–4941. [PubMed: 17664264]
13. Bitsaktsis C, Winslow G. Fatal recall responses mediated by CD8 T cells during intracellular bacteria infection. *J. Immunol.* 2006; 177:4644–4651. [PubMed: 16982903]
14. Bitsaktsis C, Huntington J, Winslow GM. Production of Interferon-g by CD4 T cells is essential for resolving ehrlichia infection. *J. Immunol.* 2004; 172:6894–6901. [PubMed: 15153508]
15. Lou DA, Hu FN. Specific antigen and organelle expression of a long-term rhesus endothelial cell line. *In Vitro Cell. Dev. Biol.* 1987; 23:75–85. [PubMed: 3102454]
16. Munderloh UG, et al. Invasion and intracellular development of the human granulocytic ehrlichiosis agent in tick cell culture. *J. Clin. Microbiol.* 1999; 37:2518–2524. [PubMed: 10405394]
17. Mix D, Winslow GM. Proteolytic processing activates a viral superantigen. *J. Exp. Med.* 1996; 184:1549–1554. [PubMed: 8879228]
18. Kurti TJ, et al. Ultrastructural analysis of the invasion of tick cells by Lyme disease spirochetes (*Borrelia burgdorferi*) in vitro. *Can. J. Zool.* 1994; 72:977–994.
19. Li JS, et al. Outer membrane protein specific monoclonal antibodies protect SCID Mice from fatal infection by the obligate intracellular bacterial pathogen *Ehrlichia chaffeensis*. *J. Immunol.* 2001; 166:1855–1862. [PubMed: 11160232]
20. Mishell RI, Dutton RW. Immunization of dissociated spleen cell cultures from normal mice. *J. Exp. Med.* 1967; 126:423–442. [PubMed: 6034749]
21. Nandi B, et al. CD4 T cell epitopes associated with protective immunity induced following vaccination of mice with an ehrlichia variable outer membrane protein. *Infect. Immun.* 2007; 75:5453–5459. [PubMed: 17698576]
22. Sotomayor EA, et al. Animal model of fatal human monocytotropic ehrlichiosis. *Am. J. Pathol.* 2001; 158:757–769. [PubMed: 11159213]

23. Munderloh UG, et al. Infection of endothelial cells with *Anaplasma marginale* and *A. phagocytophilum*. *Vet. Microbiol.* 2004; 101:53–64. [PubMed: 15201033]
24. Vachiere N, et al. Inhibition of MHC class I and class II cell surface expression on bovine endothelial cells upon infection with *Cowdria ruminantium*. *Vet. Immunol. Immunopathol.* 1998; 61:37–48. [PubMed: 9613471]
25. Singu V, Liu H, Cheng C, Ganta R. *Ehrlichia chaffeensis* expressed macrophage- and tick cell-specific 28-kilodalton outer membrane proteins. *Infect. Immun.* 2005; 73:79–87. [PubMed: 15618143]
26. Lohr CV, et al. Expression of *Anaplasma marginale* Major Surface Protein 2 operon-associated proteins during mammalian and arthropod infection. *Infect. Immun.* 2002; 70:6005–6012. [PubMed: 12379676]
27. Popov VL, et al. Ultrastructural variation of cultured *Ehrlichia chaffeensis*. *J. Med. Microbiol.* 1995; 43:411–421. [PubMed: 7473674]
28. Popov VL, et al. Ultrastructural differentiation of the genogroups in the genus *Ehrlichia*. *J. Med. Microbiol.* 1998; 47:235–251. [PubMed: 9511829]
29. Zhang JZ, et al. The developmental cycle of *Ehrlichia chaffeensis* in vertebrate cells. *Cell Microbiol.* 2007; 9:610–618. [PubMed: 16987329]

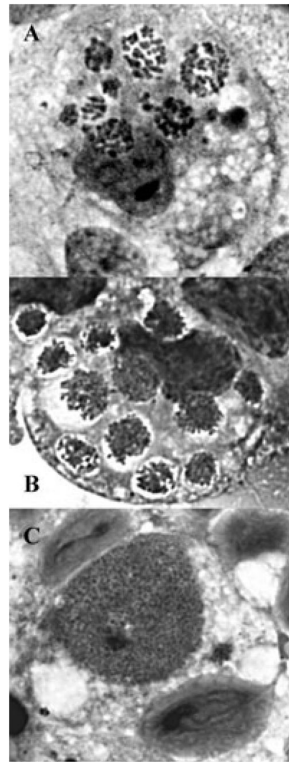


**Figure 1.**

Detection of IOE and *E. muris* in RF/6A and tick-derived ISE6 cells. Light microscopic appearance of the *Ixodes ovatus* ehrlichia in rhesus monkey endothelial cells (**A**) and ISE6 tick cells (**B**), and of *Ehrlichia muris* in ISE6 cells (**C**). Bar in C = 15  $\mu$ m. Arrow heads in **A** and **B** point to several of multiple morulae in each cell. Note the “empty” space surrounding the morulae of the *I. ovatus* ehrlichialike agent in **B**; such an appearance is also visible by phase contrast microscopy of living cultures (not shown). For comparison, panel **C** depicts *Ehrlichia muris* in ISE6 tick cell culture, typically presenting a single, large morula in one cell. N = host cell nucleus; M = morula.



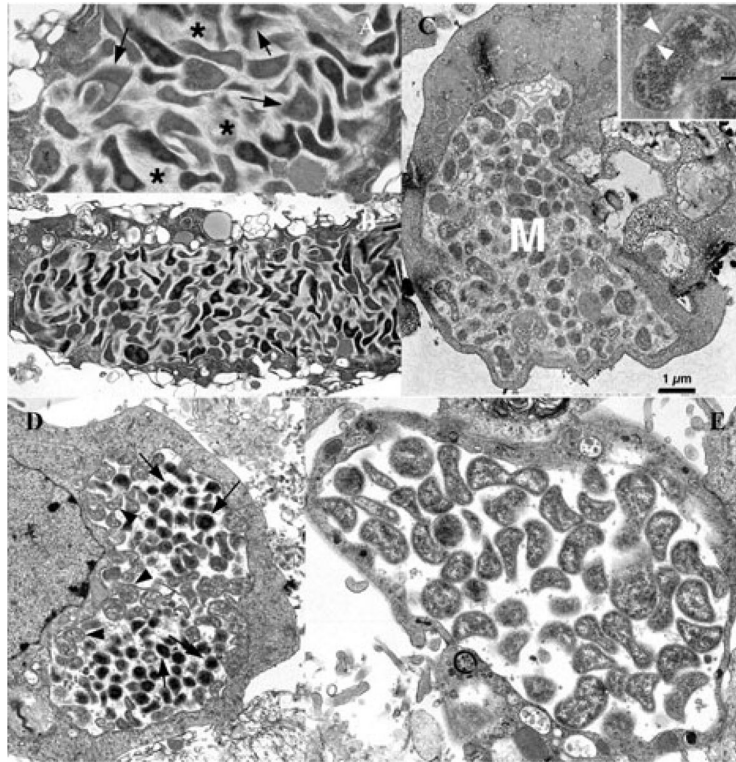


**Figure 2.** Ultrastructural analysis of IOE and *E. muris*. Panels **A** and **B**: *Ixodes ovatus* ehrlichiae in rhesus monkey endothelial cells, line RF/6A. Arrows in **A** indicate dense, fur-like material streaming from the ehrlichiae. Asterisks mark a more lightly packed fibrous substance between the bacteria. Panel **B**: Overview of *I. ovatus* ehrlichiae in cell line RF/6A. Panel **C**: Large morula (M) of the *I. ovatus* Ehrlichia-like agent in tick cell line ISE6 from *Ixodes scapularis*. **Inset**: Cross section of a single bacterium demonstrating the typical bilayer membrane structure, arrow heads. Bar = 0.1  $\mu\text{m}$ . For comparison, panels **D** and **E** depict *Ehrlichia muris* in tick cells, line ISE6. Note absence of “fur” and fibrous material in the morulae. Arrows in **D** indicate condensed bacterial cells among reticulated forms (arrow heads).

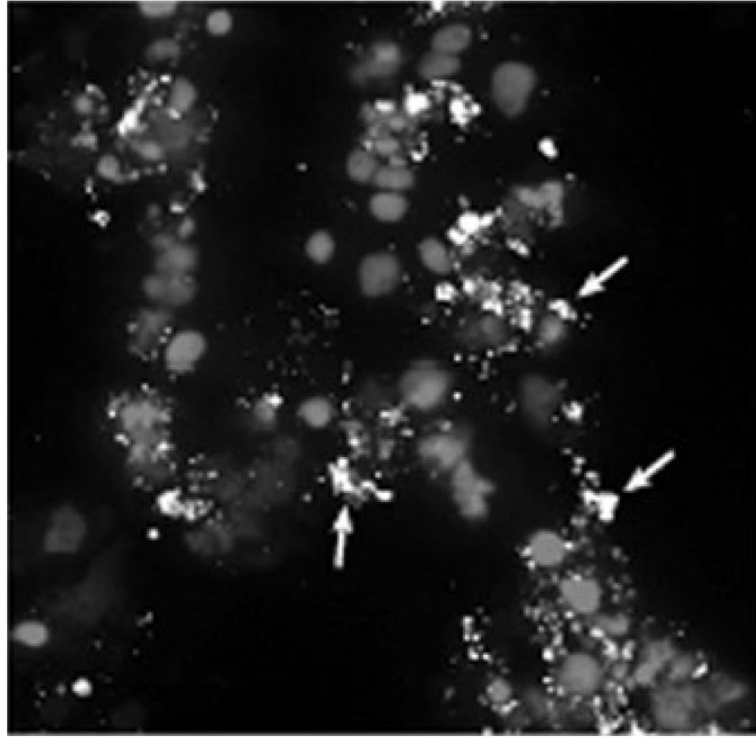


**Figure 3.** Immunofluorescence microscopy of IOE. RF/6A cells containing IOE were stained with the monoclonal antibody Ec18.1, which recognizes OMP-19. Numerous morulae can be detected in the cells (arrows).

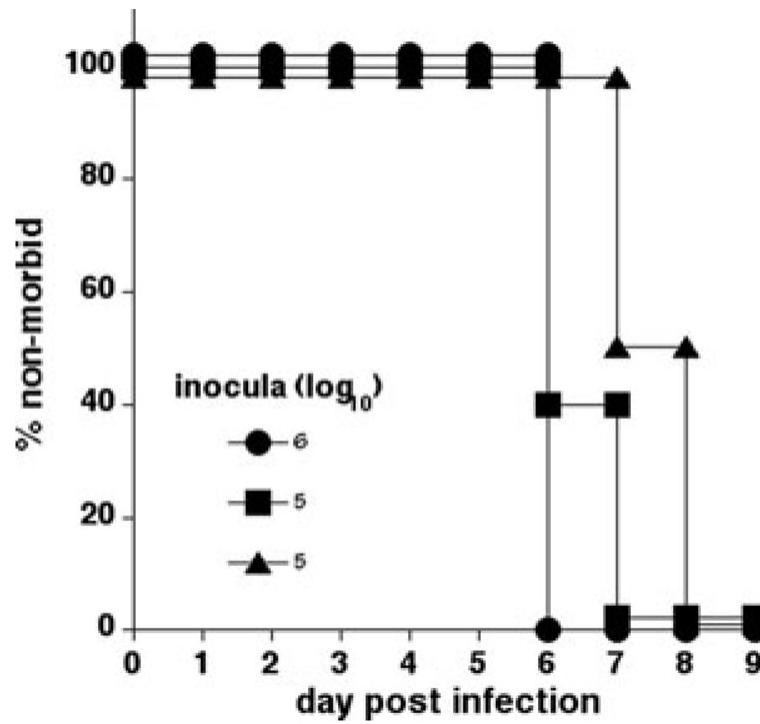


**Figure 4.** IOE cultured in RF/6A endothelial cells is fully competent to infect mice. C57BL/6 RAG-deficient mice were infected with 4–6 log<sub>10</sub> copies of IOE, via the peritoneum. Moribund mice were those judged to be incapable of surviving the infection. Three mice were used per group.